REPORT DOCUMENTATION PAGE

Form Approved
OMB No. 0704-0188

1. REPORT DATE (DD-MM-YYYY)	2. REPORT TYPE	3. DATES COVERED (From - To)
31-01-2008	Final	01/01/04 - 12/31/06

4. TITLE AND SUBTITLE
Experimental Studies of Transitional Boundary Layer Shock Wave Interactions

5a. CONTRACT NUMBER

5b. GRANT NUMBER
FA9550-04-1-0112.

5c. PROGRAM ELEMENT NUMBER

6. AUTHOR(S)
N.T. Clemens, D.S. Dolling, Z.R. Murphree and K.B. Yüceil

5d. PROJECT NUMBER

5e. TASK NUMBER

5f. WORK UNIT NUMBER

7. PERFORMING ORGANIZATION NAME(S) AND ADDRESS(ES)
Center for Aeromechanics Research. The Universitv of Texas at Austin

8. PERFORMING ORGANIZATION REPORT NUMBER
None

9. SPONSORING / MONITORING AGENCY NAME(S) AND ADDRESS(ES)
Air Force Office of Scientific Research
875 North Randolph Street, Room 3112
Arlington, VA 22203
Dr John Schmisseur/NA

10. SPONSOR/MONITOR'S ACRONYM(S)
AFOSR

11. SPONSOR/MONITOR'S REPORT NUMBER(S)
AFRL-SR-AR-TR-08-0109

12. DISTRIBUTION / AVAILABILITY STATEMENT
Approved for public release,
distribution unlimited

13. SUPPLEMENTARY NOTES

14. ABSTRACT
Transitional shock wave / boundary layer interactions are studied with planar imaging techniques. The interaction is generated by a cylinder mounted on a flat plate in a Mach 5 flow. Planar laser scattering (PLS) and particle image velocimetry (PIV) are used to visualize the flow structure. Images are obtained in streamwise-spanwise planes (plan view). Earlier work focused on investigating similar interactions with tripped boundary layers, whereas the current work focuses on the case where transition occurs naturally.. One goal of this preliminary study was to see if repeatable interactions could be generated.. Imaging was conducted for three downstream locations of the cylinder. The PLS imaging revealed that the transitional interactions resulting from an untripped boundary layer are similar to those generated by tripping. In general it is observed that the separated flow region of transitional interactions exhibits larger variations in their scale and shape than fully turbulent interactions. When the cylinder is farthest upstream (5.3 diameters from leading edge) two types of separation shock are seen: an apparently laminar shock along the plate centerline and a turbulent one in the outboard region. As the cylinder is moved downstream (10.7 diameters), this dual structure is not as apparent, which is consistent with the upstream boundary layer becoming more turbulent. Finally, at 16 diameters downstream the interaction exhibits extreme variations in its shape, which we believe to be caused by sidewall interference. The PIV measurements largely confirm these qualitative observations.

15. SUBJECT TERMS
Transitional boundary layers, unsteady separated flow, shock wave

16. SECURITY CLASSIFICATION OF:			17. LIMITATION OF ABSTRACT	18. NUMBER OF PAGES	19a. NAME OF RESPONSIBLE PERSON
a. REPORT	b. ABSTRACT	c. THIS PAGE			David S Dolling
Unclassified	Unclassified	Unclassified		14	19b. TELEPHONE NUMBER (include area code) 512 471-4470

Experimental Studies of Transitional Boundary Layer Shock Wave Interactions

Final Report for the period 1 January, 2004 - 31 December, 2006
Grant FA9550-04-1-0112

D. S. Dolling
Principal Investigator
Report Authors (N.T. Clemens, D.S. Dolling, Z.R. Murphree, and K.B. Yüceil)
Center for Aeromechanics Research, WRW 220
Department of Aerospace Engineering & Engineering Mechanics
The University of Texas at Austin
Austin, Texas 78712-1085
Telephone: (512) 471-4470
FAX: (512) 475-6743
e-mail: ddolling@mail.utexas.edu

Abstract: Shock wave / boundary layer interactions, where the upstream boundary layer is transitional, are studied with planar imaging techniques. The interaction is generated by a cylinder mounted on a flat plate in a Mach 5 flow. Planar laser scattering (PLS) from a seeded alcohol fog and particle image velocimetry (PIV) are used to visualize the flow structure. Images are obtained in streamwise-spanwise planes (plan view). Earlier work focused on investigating similar interactions with tripped boundary layers, whereas the current work focuses on the case where transition occurs naturally on the plate without tripping. One goal of this preliminary study was to see if repeatable interactions could be generated under these conditions. Imaging was conducted for three downstream locations of the cylinder. The PLS imaging revealed that the transitional interactions resulting from an untripped boundary layer are similar to those generated by tripping. In general it is observed that the separated flow region of transitional interactions exhibits larger variations in their scale and shape than fully turbulent interactions. When the cylinder is farthest upstream (5.3 diameters from leading edge) two types of separation shock are seen: an apparently laminar shock along the plate centerline and a turbulent one in the outboard region. As the cylinder is moved downstream (10.7 diameters), this dual structure is not as apparent, which is consistent with the upstream boundary layer becoming more turbulent. Finally, at 16 diameters downstream the interaction exhibits extreme variations in its shape, which we believe to be caused by sidewall interference. The PIV measurements largely confirm these qualitative observations.

Nomenclature

d	=	cylinder diameter
X_{cyl}	=	distance from plate leading edge to cylinder leading edge
X_{sep}	=	distance from plate leading edge to primary separation line along plate centerline
X_{trans}	=	distance from plate leading edge to transition along plate centerline
λ_{sep}	=	distance from cylinder leading edge to primary separation line along plate centerline

I. Introduction

Shock wave/boundary layer interaction (SWBLI), often accompanied by separation, is a commonly occuring feature of high-speed flight, and has been the focus of extensive research. Most of the work that has been done in the SWBLI field over the past 50 years has been in fully-developed turbulent flows as most applications where one would find these interactions were at transonic and low supersonic speeds at altitudes where Reynolds numbers are large and turbulent flow the norm. Numerous review articles have been written on turbulent interactions[1-11], and more recently reviews of papers in the field have focused on the interaction unsteadiness and its cause(s).[7, 12, 13] An understanding of these turbulent interactions is very important for vehicle design because the interactions result in very high unsteady thermal and acoustic loads that can result in diminished component performance and material failure. Laminar interactions are relatively rare, and are for the most part steady, and with modern computing power can be modeled with sufficient accuracy for most engineering applications[14] (unless the flow is a special case, e.g. with chemistry). In contrast, transitional shock wave/boundary layer interactions, in which the incoming boundary layer is in a transitional state, or in which transition is induced within the interaction itself, have received little attention. This lack of attention has stemmed from both a lack of critical applications and from the formidable challenges that the study of such flows poses to both experiment and computation.

In spite of the recent increase in interest in this topic, it is fair to say that our current understanding of transitional interactions is extremely poor. Although experimental data from past studies are limited, there are a number of important observations that have been made regarding transitional interactions. In one of the earliest studies, Chapman, Keuhn and Larson[15] found that the pressure distribution depended mainly on the location of transition relative to that of separation and reattachment. This study was also the first to look at the length scales of the interaction. The highly unsteady nature of transitional interactions relative to that of turbulent interactions was found when Chapman et al. looked at high speed movies of the interactions. The results of this study also seemed to suggest that the length scales of the unsteadiness were also larger for the transitional case as compared to the turbulent, which was further supported by the work of Korkegi and Morton with hemicylindrically blunted fins.[16] Young et al.[17] found an interesting difference between schlieren images of transitional and turbulent interactions. In the turbulent case they noted a single "well-defined separation shock", but in the transitional case "multiple separation shocks" were observed.

As mentioned above, the length scales of the SWBLI depend on the boundary layer regime where the interaction is occurring. In a fully laminar interaction of a circular cylinder on a flat plate, the separation line can occur in a

range from 7-12 cylinder diameters (d) depending on how the separation is measured. The larger values (9-12d) are obtained when the separation point is defined by a rise in surface temperature or static pressure[14] over the undisturbed values, but these measurements generally overpredict the separation distance because separation can occur several cylinder diameters downstream of the first pressure rise.[18] In the turbulent regime the interaction scales are much smaller; generally the separation distance is 2-3d.[19]

Previous studies in our facility of transitional interactions are largely consistent the previous work described above.[20] In this previous work Mach 5 interactions were generated with a circular cylinder mounted on a flat plate that itself was mounted in the center of the test section. Different types of interactions were generated by moving the cylinder to different streamwise locations on the plate. For example, a set of surface streakline visualizations is shown in Figure 1, where the cylinder is at three different locations. The flow is from top to bottom. These images illustrate the difference in both shape and scale of three interaction regimes: "fully turbulent", "transitional" and "laminar-transitional". These results also agreed well with those of Kaufmann et al.[21] as plotted in Fig. 2. The separation distance (λ_{scp}) is normalized by the cylinder diameter, and the location of separation from the plate leading edge (X_{scp}) is normalized by the downstream end of the transition band (X_{trans}) as predicted by a correlation from Ramesh and Tannehill.[22] Our previous study also used 10 kHz PLS to show that the transitional interaction is indeed highly unsteady, especially near the laminar side of transition, and that this unsteadiness decreases to the turbulent level as the cylinder is moved downstream through the transitional band.

A major limitation of our previous study is the flow visualization was carried out on transitional interactions that had tripped boundary layers. The concern is that the results may have been dependent on the nature of the trip that was used. Therefore, the aim of the current work is to conduct an experimental investigation of cylinder-induced interactions in a Mach 5 flow where the upstream boundary layer undergoes natural transition. Since natural transition takes longer to develop, a concern was whether transitional interactions could be obtained before sidewall disturbances contaminated the flow. Furthermore, in the current work, both planar laser scattering (PLS) from a condensed alcohol fog and particle image velocimetry (PIV) were used to investigate the flow structure. The measurements were made in streamwise-spanwise planes (plan view) so that the global structure of the interactions could be observed. The PLS imaging was conducted in double-pulse mode (25 μs between images) so that some time dependent information could be obtained. The objective is to characterize the overall flow structure of the transitional interactions for different downstream locations of the cylinder.

II. Experimental Program and Techniques

The experimental program is carried out in the Mach 5 blow down wind tunnel located at the High-Speed Wind Tunnel Laboratory at the Pickle Research Campus of The University of Texas at Austin. The facility uses eight tanks that have a combined storage volume of 140 ft^3 and are pressurized to a maximum of 2500 psia. The stagnation temperature and pressure are 580° R and 360 psia. Typical run times are about 20 seconds. The unit Reynolds number in the test section is 35×10^6 m^{-1}. Downstream of the 2-D Mach 5 nozzle, the flow enters a 27 *in* long constant area test section which is 7 *in* high and 6 *in* wide. The interactions are generated on a 10 *in* long flat plate mounted at the centerline of the test section. The plate was mounted to the sidewalls and does not use a strut in order to minimize wind tunnel blockage. A single circular cylinder, of diameter 3/8 *in*, was used to produce the shock wave/boundary layer interactions as shown in Fig. 3. The cylinder was mounted on the surface of the plate with a screw jack which permits the cylinder to be moved in the streamwise direction. This mounting mechanism was used because it allows for the cylinder to be placed at different streamwise locations on the plate without having threaded holes on the surface of the plate, thereby eliminating the flow disturbances that such holes might cause. The plate was painted black to reduce background reflections of the laser light used to visualize the flow. The painted surface was then sanded with fine grit sandpaper to a smooth polished finish. In the current study the cylinder was placed at three different locations along the plate: 2.8, 4.0 and 6.0 inches from the leading edge of the plate.

Two laser diagnostic techniques were employed in this study: plaser laser scattering (PLS) from a condensed alcohol fog and particle image velocimetry (PIV). In PLS, which is used for flow visualization, the flow is seeded with a finely atomized ethanol spray upstream of the stagnation chamber. As the aerosol travels to the nozzle it evaporates, but then re-condenses into a fine fog as it is expands through the nozzle. Laser light is scattered from the fog in order to visualize the flow. The light source for the PLS was an Nd:YAG laser (Spectra-Physics PIV 400), frequency doubled to 532 nm. The repetition rate of the laser was 10 Hz, the typical pulse energy was about 35 mJ and the pulse duration was 10 ns. The light was formed into a sheet and brought into the test-section parallel to plate as shown in Fig. 4. The laser sheet was located 2 mm from the plate surface and was about 125 mm in width. The

scattered light was imaged with a 1k×1k CCD camera (Kodak Megaplus ES1.0). In some of the cases, double-pulse images were obtained by acquiring two rapid images in rapid succession (25 μs between images). This was done by double-pulsing the laser and capturing the images using the frame straddling capability of the ES1.0 camera. These double pulsed image pairs were acquired at a framing rate of 10 Hz.

Previous work has shown that the ethanol fog droplets that are formed small enough (<0.2 μm) to faithfully track the motion of the flow. In regions of high temperature, such as in a boundary layer or region of separated flow, the ethanol will evaporate and the scattering intensity will decrease. In regions of high density, such as on the downstream side of a shock wave, the scattering intensity increases because of an increase in the particle number density. For very strong shocks, the temperature rise is so large that the fog evaporates. This discussion shows that the PLS signals are dependent on a complex number of factors and so must be interpreted with caution.

The PIV technique, from which velocity data were obtained, used the same laser and camera setup, as described above. For PIV the flow was seeded in the stagnation chamber with titanium-dioxide particles that have a nominal primary particle diameter of 20 nm. Experiments by Hou[23] determined the particle response time of these same particles (delivered with the same seeder as in the current study) by imaging their velocity as they passed through a normal shock. These measurements showed that the particle response time was less than 3 μs. This response time is consistent with particles that are about 0.26 μm in diameter, which shows that the primary particles have agglomerated significantly. For the PIV the laser sheet was also oriented parallel to the plate to enable "plan view" (streamwise-spanwise) velocity fields to be obtained. Particle image pairs were acquired by frame straddling the Kodak ES1.0 camera with resolution of 1024 by 1024 pixels. The time delay between the first and second images of each pair was 2 microseconds, and the pairs were acquired at a framing rate of 10 Hz. These image pairs were then processed with commercially available PIV software (TSI Insight 6.1) to obtain vector fields. The PIV interrogation window was 32×32 pixels, which gave resolution per window of 2.8 mm. For PIV the energy per pulse was 45 mJ and the sheet height was 3mm.

III. Results

PLS images were acquired at downstream locations of 2.8, 4.0 and 6.0 *in* from the leading edge of the plate to the leading edge of the cylinder. These distances correspond to 5.3*d*, 10.7*d* and 16*d*, respectively, where *d* is the cylinder diameter. Figure 5 shows sample PLS images for the case where the cylinder is 2.8 *in* from the leading edge. Figure 5a and 5b show two examples of double-pulse image pairs where the time delay was 25 μs. The field of view is 3.4 inches in the streamwise direction and the flow is from left to right in the figure. The cylinder can be seen at the right hand edge of the image. The laser sheet passed just in front of the cylinder and the field of view extends to 0.35 *in* upstream of the plate leading edge. The plate leading edge causes strong scattering of the laser light and so is seen as a white vertical line at the left of the image. In the figure, high-signal white regions correspond to regions of high fog density. Light streaks are observed in the freestream, which is caused by pockets of nonuniform seeding that are stretched out as they expand through the nozzle. The separation region can be seen as the black area in the region surrounding the cylinder. The separated flow is black because the low-velocity fluid is relatively warm and so evaporates the fog particles. The separation shock is a more subtle feature, but it can be seen as a bright band just upstream of the separation line. The separation line is here assumed to be the farthest upstream extent of the separation region.

The shape of the separated flow is consistent with what is known about transitional interactions, as inferred from previous surface flow visualization studies; however, the scale of the separated flow seems to be smaller than expected. The separated flow scale in Fig. 5 is about 2-3 diameters, which is more consistent with a turbulent than a transitional interaction. However, it should be emphasized that the laser sheet is 2 mm from the surface of the plate and so the actual start of separation is likely farther upstream. In other words, the visualizations reveal the location where the separated flow bulges out past the location of the laser sheet. Furthermore, in Fig. 5b, the separation shock (see label) is seen to be nearly 0.4 *in* farther upstream than the separated flow. Obviously, the separation shock is present because the flow is separated. If we assume the separation shock is at the Mach angle of about 12 degrees, then this means separation starts about 0.6 *in* upstream of the separation shock or up to 5 diameters upstream of the cylinder. This discussion shows that the separation scale may not after all be inconsistent with expectations.

As stated above, the shape of the separated flow envelope is similar to what has been observed with surface streakline visualization. The images reveal the larger scaling of the separated flow directly upstream of the cylinder (i.e., a larger radius of curvature) and greater sweepback of the outboard regions. Between these inboard and outboard regions is an inflection point in the separation line that is particularly characteristic of transitional interactions. The clearest example of this type of structure is the right image of Fig. 5b. At this time it is not entirely clear what causes this behavior, but it could be a result of the spatial development of transition on the plate. In other

words, the inboard region may reflect more of a laminar separation process, whereas the outboard regions, which are spatially farther downstream, may reflect a more turbulent separation. Other observations that can be made from Fig. 5 is that in Fig. 5a the separation shock near the centerline is very close to the separated flow, but in Fig. 5b the shock is farther upstream of the separation region. What may be a related observation, and which is particularly clear in Fig. 5b, is that near the centerline there is a larger distance between the separation shock and the separation region as compared to outboard regions. The reason for this is not clear, but it does suggest a difference in the separation process, such as was described above; i.e., on centerline the separation may occur with a more laminar boundary layer. At this time, however, this is largely conjecture and will be a topic of further investigation.

Another feature that can be observed in Fig. 5 is the presence of streamwise streaks seen at the upstream edge of the separation region. Although it is possible that these streaks arise from the upstream boundary layer, it is more probable that they are the signature of Göertler vortices that form in the presence of the concave streamline curvature associated with separation.

The double-pulse imaging enables a limited investigation into the unsteady characteristics of the interaction. A careful viewing of the double-pulse pairs shows that substantial changes can occur to the shape of the separated flow over 25 microseconds. Since the laser sheet is largely above the height of the boundary layer, however, it is not known if upstream boundary layer fluctuations are responsible for the changes. More will be discussed on this point when we discuss the cases where the cylinder is farther downstream.

Figure 6 shows two sample double-pulse pairs for the case where the cylinder is location at 4.0 *in* downstream of the leading edge. The interaction changes in some respects. First of all, the separation shock (seen as the white fringe upstream of the separated flow) is at all spanwise locations very close to the separation region. Recall that the previous case showed that near the centerline the separation shock was much more separated from the separated flow. The fact that the separation shock is everywhere close suggests that the boundary layer is more turbulent at all spanwise locations.

Another observation that can be made for this case is that small disturbances in the upstream boundary layer can be seen. These disturbances, which are a result of boundary layer transition, show up as dark spots, such as seen in Fig. 6a (left) on centerline just upstream of the separated flow. One interesting aspect of these spots is that on the scale of the 25 microsecond time delay, the location where the spots appear in the image seems to remain constant. In other words, as individual spots convect downstream new spots appear where the old spots were. The laser sheet is 2mm above the surface of the plate, which is above the boundary layer height, and so these spots are likely present farther upstream but we are not able to image them due to the sheet location. In Figure 6 these spots are seen to convect through the interaction in each image pair. Figure 6a shows a number of small spots propagating into the interaction, whereas Fig. 6b shows the effect of a single large spot (seen just upstream of the separation region). The time delay between image pairs is again 25 microseconds. It can be observed, particularly by flipping back and forth between images on a computer screen, that as the spots propagate through the interaction, the separated flow scale increases. This observation is consistent with what might be expected of the effect of velocity fluctuations on a separated flow because the spots are associated with slower moving fluid (slower moving fluid is warmer according to the energy equation), and this may cause a less full velocity profile that is less resistant to separation.

Figure 7 shows PLS images of the interaction with the cylinder at 6.0 *in* downstream of the leading edge. These images are not double-pulsed, but are single images taken at 10Hz. According to both our previous work and the Ramesh and Tannehill[22] correlation, the boundary layer at this streamwise location should be turbulent. Our previous work showed that the unsteadiness of the transitional interaction decreases as the cylinder is moved downstream. This is not to say that the turbulent interaction is steady, which is certainly not the case, but at 6 inches it was expected that the interaction would be steadier than the transitional cases. This was not what was observed as seen in Fig. 7. Not only was the interaction highly unsteady, but the shape of the interaction was extremely variable and was not consistent with previous work. For example, in Fig. 7 the interaction in the upper left image looks like a classical turbulent case, however, the other images show that the separated flow shape is highly variable. Figure 7 lower left is particularly strange because the separated flow appears almost pointed, and at lower right the outboard region of the separated flow is not swept at all but is parallel to the flow direction. One clue to this strange behavior is that whenever these very strange interaction shapes occur, the upstream flow (as visualized by the streaks in the fog) seems to be highly perturbed. For example, Fig. 7 upper right shows a case where the fog streaklines seem to be deflected inward toward the centerline of the tunnel. This will be discussed further when we consider the PIV data.

PIV data were taken with the cylinder at the same nominal streamwise distances and with the same nominal field of view. Obtaining adequate seeding density for the PIV proved to be a difficult challenge. It was found that seeding conditions that worked well at Mach 2 were inadequate at Mach 5. At Mach 5, the flow undergoes such large flow expansion that the seeding density in the plenum has to be of order 100 times larger than that desired in the test

section. To accomplish this, modifications to the seeder piping was made and much higher seeding flow rates were used than in our previous work.

Figure 8 shows four sample u-velocity contours plots for the case where the cylinder was placed at x=6.0 inches. Note that these images were not acquired simultaneously with the PLS imaging. The red region in the image represents the upstream freestream whose velocity is relatively uniform. Recall that the laser sheet is above the boundary layer. The velocity contours do reveal, however, that the separated flow region is indeed a region of low velocity. Interestingly, the separated flow region (blue) is seen to exhibit strong similarity to what was inferred to be the separated flow region in the PLS imaging. Since the PLS signal is dependent on condensation/evaporation processes, it could potentially lead to inaccurate inferences about the physical flow structure. The PIV confirms, however, that the previous observations of the separated flow structure are sound. Figure 8 shows the same types of widely varying separated flow shapes. The upper left plot shows a more conventional interaction, whereas the upper right and lower left plots reveal the very broad shape shown in Fig. 7. The very broad shapes of the separated flow indicate that separation is occurring across the entire width of the field of view without being swept back in some cases. We believe that this confirms that sidewall interactions are influencing the flow at this location. We note that our previous work shows that turbulent interactions (tripped) do not have this same sidewall effect at this location. It is likely that the transitional interactions, because of the more massive separation, present a larger disturbance to the flow. The larger disturbance may lead to stronger separation of the sidewall boundary layers and hence stronger sidewall influence. Since we desire to study the downstream evolution of transitional interactions, future work will be aimed at redesigning the centerplate to reduce the magnitude of this effect.

IV. Conclusion

An exploratory study was conducted of shock wave / boundary layer interactions, where the upstream boundary layer is undergoing transition. The flow was studied by using two imaging techniques: PLS from a condensed alcohol fog and PIV. The Mach 5 cylinder interaction was generated in a conventional blow down tunnel. The goal of this work is to determine how the structure and unsteady characteristics of transitional interactions differ from their turbulent counterparts. This current study differed from our previous work in this area in that the upstream boundary layer underwent natural transition. The PLS imaging revealed that the transitional interactions resulting from an untripped boundary layer are similar to those generated by tripping. In general it is observed that the separated flow region of transitional interactions exhibits larger variations in their scale and shape than fully turbulent interactions. When the cylinder is farthest upstream (5.3 diameters from leading edge) two types of separation shock are seen: an apparently laminar shock along the plate centerline and a turbulent one in the outboard region. As the cylinder is moved downstream (10.7 diameters), this dual structure is not as apparent, which is consistent with the upstream boundary layer becoming more turbulent. Finally, at 16 diameters downstream the interaction exhibits extreme variations in its shape, which we believe to be caused by sidewall interference. The PIV measurements largely confirm these qualitative observations.

The double-pulse PLS imaging provides some new insight into the unsteady characteristics of the interactions. Turbulent spots could be clearly seen to convect into the interaction and affect its structure. When the turbulent spots convect through the interaction, the separation region is seen to respond by locally growing and moving upstream. The PLS further showed that a more laminar interaction exhibits a separation shock that is relatively far upstream of the separated flow. In contrast, more turbulent interactions exhibit separation shocks that are on the upstream edge of the separation region. In general, the more turbulent the interaction is, the closer the separation shock is to the separation region. It is possible that differences in the separation processes might explain the differences between the inboard and outboard length scales of the interaction, but this phenomenon requires more study.

PIV also proved to be a valuable for validating, in a quantitative way, what was observed with PLS. The instantaneous and average vector fields complement the PLS results, giving a clearer picture of what is happening in the interaction. Both PLS and PIV show that the interaction suffers from significant sidewall effects when the cylinder is at its farthest downstream location (x=16d). This shows the difficulty in studying transitional interactions when the boundary layer undergoes natural transition. Future work will focus on obtaining both velocity data in the separated flow region and better temporal and spatial resolution of the velocity field.

Acknowledgments

The authors would like to thank Dr. Bharath Ganipathisubramani, Justin Wagner, Mirko Gamba and Agustin Valdivia for their help with the experimental setup and execution, and Edward J. Zihlman and Donna Soward for their help and patience. The views and conclusions contained herein are those of the authors and should not be

interpreted as necessarily representing the official policies or endorsements, either expressed or implied, of the Air Force Office of Scientific Research or the U.S. Government.

References

[1]Green, J. E., "Interactions Between Shock Waves and Turbulent Boundary Layers," *Progress in Aerospace Sciences*, Vol. 11, Pergamon Press, 1970, pp. 235-340.

[2]Korkegi, R., "Survey of Viscous Interactions Associated with High Mach Number Flight," *AIAA Journal*, Vol. 9, May 1971, pp.771-784.

[3]Stanewsky, E., "Shock-Boundary Layer Interaction in Transonic and Supersonic Flow," von Kármán Institute Lecture Series-59, von Kármán Institute, Brussels, Belgium, 1973.

[4]Hankey, W. L., Jr., and Holden, M. S., "Two-Dimensional Shock-Wave Boundary Layer Interactions in High Speed Flows," AGARDograph No. 203, 1975.

[5]Délery, J., and Marvin, J., "Shock-Wave Boundary-Layer Interactions," AGARDograph No. 280, Feb. 1986.

[6]Settles, G. S., and Dolling, D. S. "Swept Shock-Wave/Boundary Layer Interactions," in Tactical Missile Aerodynamics: General Topics, *AIAA Progress in Astronautics and Aeronautics*, Vol. 141, 1992, pp.505-574

[7]Dolling, D. S., "Fluctuating Loads in Shock Wave/Turbulent Boundary Layer Interaction: Tutorial and Update," AIAA Paper 93-0284, January 1993.

[8] Délery, J., and Panaras, A., "Shock-Wave Boundary-Layer Interactions in High Mach Number Flows," AGARD AR-319, Vol. 1, May 1996.

[9]Zheltovodov, A., "Shock Waves/Turbulent Boundary Layer Interactions – Fundamental Studies and Applications," AIAA Paper No. 96-1977, 1996

[10]Smits, A. J., and Dussuage, J. P., "Turbulent Shear Layers in Supersonic Flow," New York, American Institute of Physics Press from Springer-Verlag, 1998.

[11]Knight, D. D., and Degrez, G., "Shock Wave Boundary Layer Interactions in High Mach Number Flows. A Critical Survey of Current Numerical Prediction Capabilities," AGARD Advisory Report 319, Vol. II, pp.1.1-1.36, December 1998.

[12]Beresh, S. J., "The Effect of the Incoming Boundary Layer on a Shock-Induced Separated Flow Using Particle Image Velocimetry," Ph-D dissertation, Department of Aerospace Engineering and Engineering Mechanics, The University of Texas at Austin, Austin, Texas, August 1999.

[13]Ganapathisubramani, B., Clemens, N.T., Dolling, D.S., "Planar Imaging Measurements to Study the Effect of Spanwise Structures of Upstream Turbulent Boundary Layer On Shock Induced Separation," *44th Aerospace Sciences Meeting and Exhibit, Reno, Nevada, January 9th-12th, 2006*, AIAA 2006-0324.

[14]Hung, F.T. and Clauss J.M., "Three-Dimensional Protuberance Interference Heating in High-Speed Flow," AIAA-80-0289, AIAA 18th Aerospace Sciences Meeting, Jan 1980.

[15]Chapman, D. R., Kuehn, D. M., and Larson, H. K., "Investigation of Separated Flows in Supersonic and Subsonic Streams with Emphasis on the Effect of Transition," NACA Report 1356, 1958.

[16] Kaufman, L. G., II, Korkegi R. H. and Morton, L. C., "Shock Impingement Caused By Boundary Layer Separation Ahead of Blunt Fins," ARL 72-0118, Aerospace Research Laboratories, Wright-Patterson Air Force Base, Ohio, Aug 1972.

[17]Young, F.L., Kaufman, L.G., and Korkegi, R.H., "Experimental Investigation of the Interactions Between Blunt Fin Shock Waves and Adjacent Boundary Layers at Mach Numbers 3 and 5," ARL 68-0214, Dec 1968.

[18]Özcan O. and Holt M. (1984), "Supersonic Separated Flow past a Cylindrical Obstacle on a Flat Plate," *AIAA Journal*, Vol. 22 No. 5, pp. 611-617.

[19]Dolling, D. S., and Bogdonoff, S. M., "Scaling of Interactions of Cylinders with Supersonic Turbulent Boundary Layers," *AIAA Journal*, (AIAA 81-4110), Vol. 19, No. 5, p. 655, May 1981.

[20]Murphree, Z., Jagodzinski, J., Clemens, N., Dolling, D., "Experimental Studies of Transitional Boundary Layer Shock Wave Interactions" *44th Aerospace Sciences Meeting and Exhibit, Reno, Nevada, January 9th-12th, 2006*, AIAA 2006-0326.

[21] F.L., Kaufman, L.G., and Korkegi, R.H., "Experimental Investigation of the Interactions Between Blunt Fin Shock Waves and Adjacent Boundary Layers at Mach Numbers 3 and 5," ARL 68-0214, Dec 1968.

[22]Ramesh, M. D. and Tannehill J. C., "Correlations To Predict Transition In Two-Dimensional Supersonic Flows," 33rd AIAA Fluid Dynamics Conference and Exhibit, June 23-26.

[23]Hou, Y. X., *Particle Image Velocimetry Study of Shock Induced Turbulent Boundary Layer Separation*, Ph.D. thesis, Department of Aerospace Engineering and Engineering Mechanics, The University of Texas at Austin, Texas, USA, 2003.

Figures

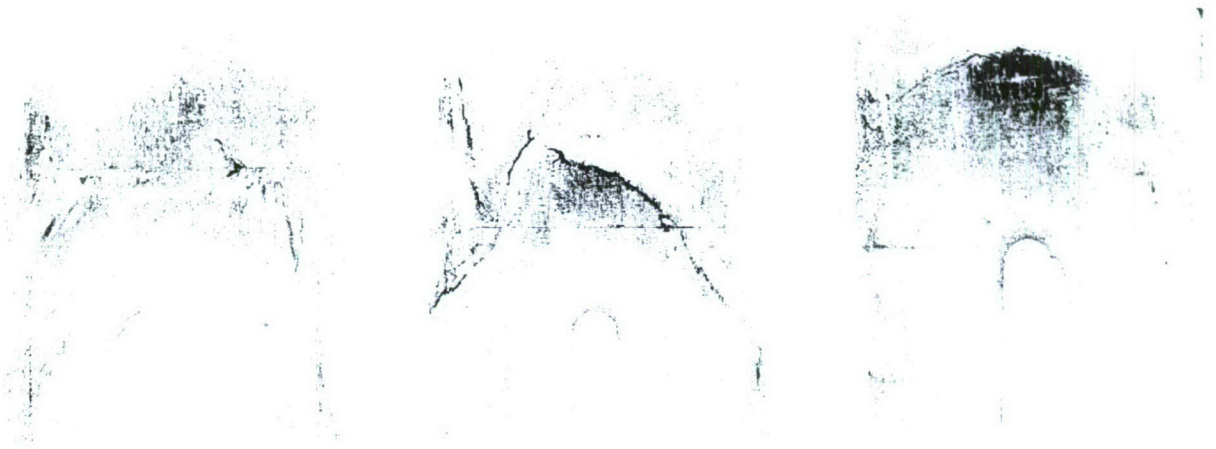

Figure 1. Surface streakline visualization (kerosene-lampblack) of cylinder-induced interactions in a Mach 5 flow. ***(a) "Fully turbulent": X_{cyl} = 5 in, (b) "transitional": X_{cyl} = 4 in, and (c) "laminar": X_{cyl} = 2.75 in.***

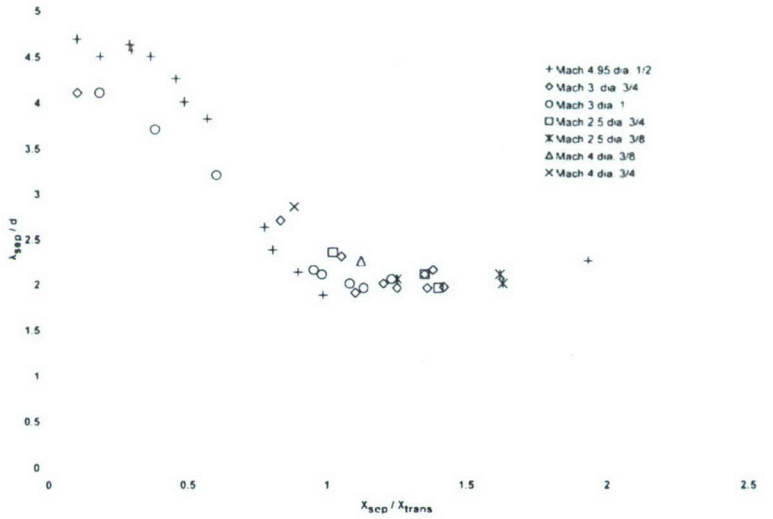

Figure 2. Comparison of data from current study with that of Kaufman et al. [4]

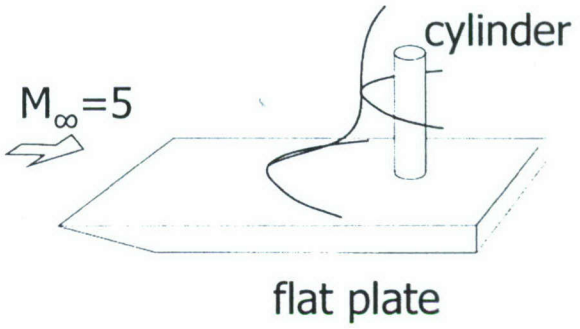

Figure 3. Schematic of interaction generating model.

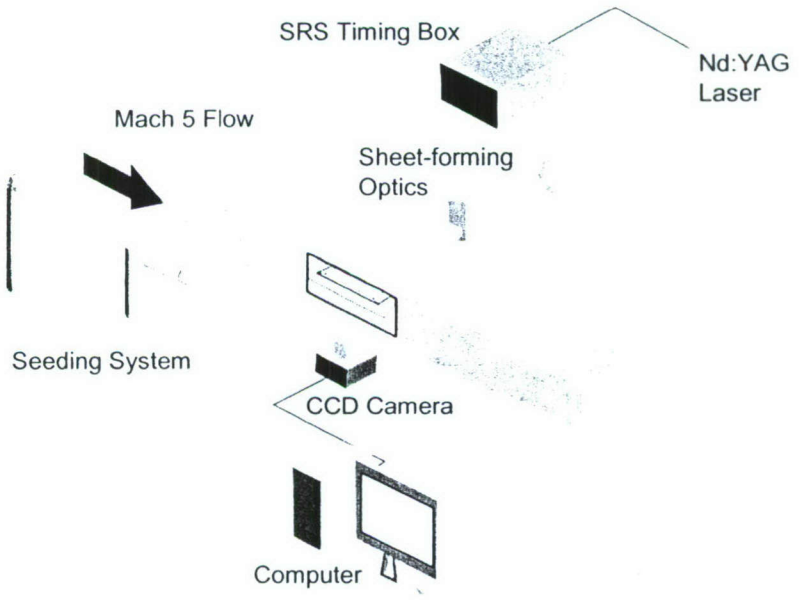

Figure 4. Schematic diagram of PLS and PIV setup.

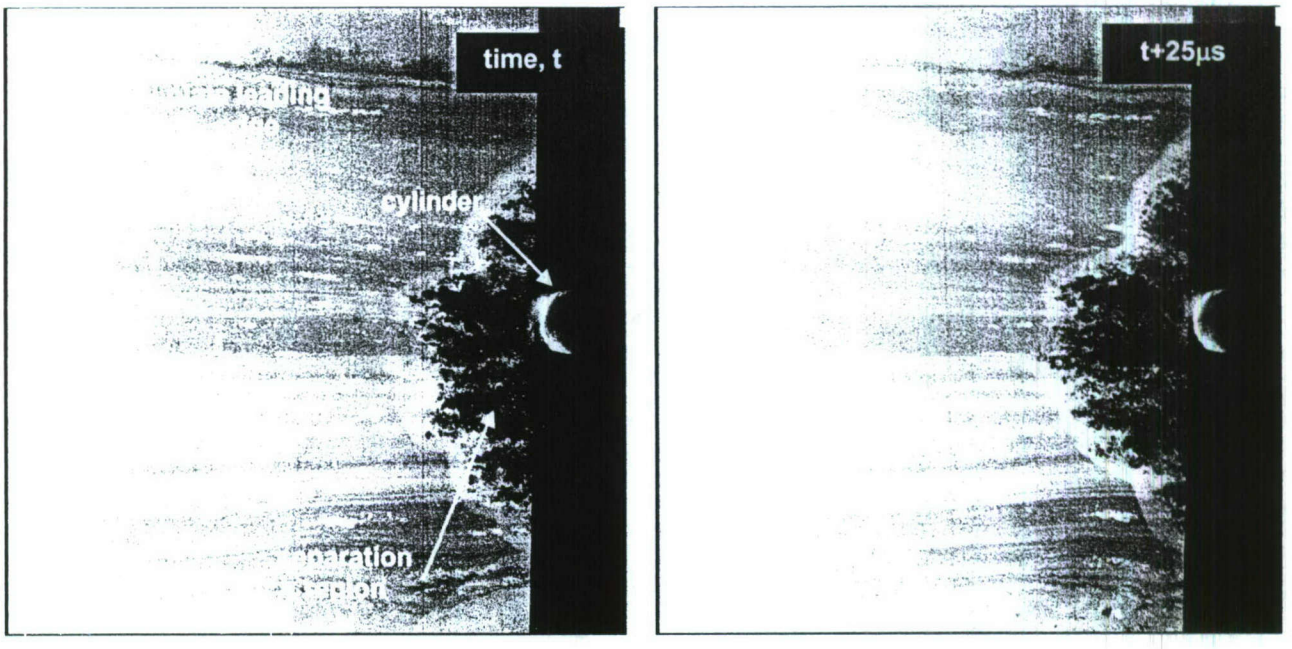

(a)

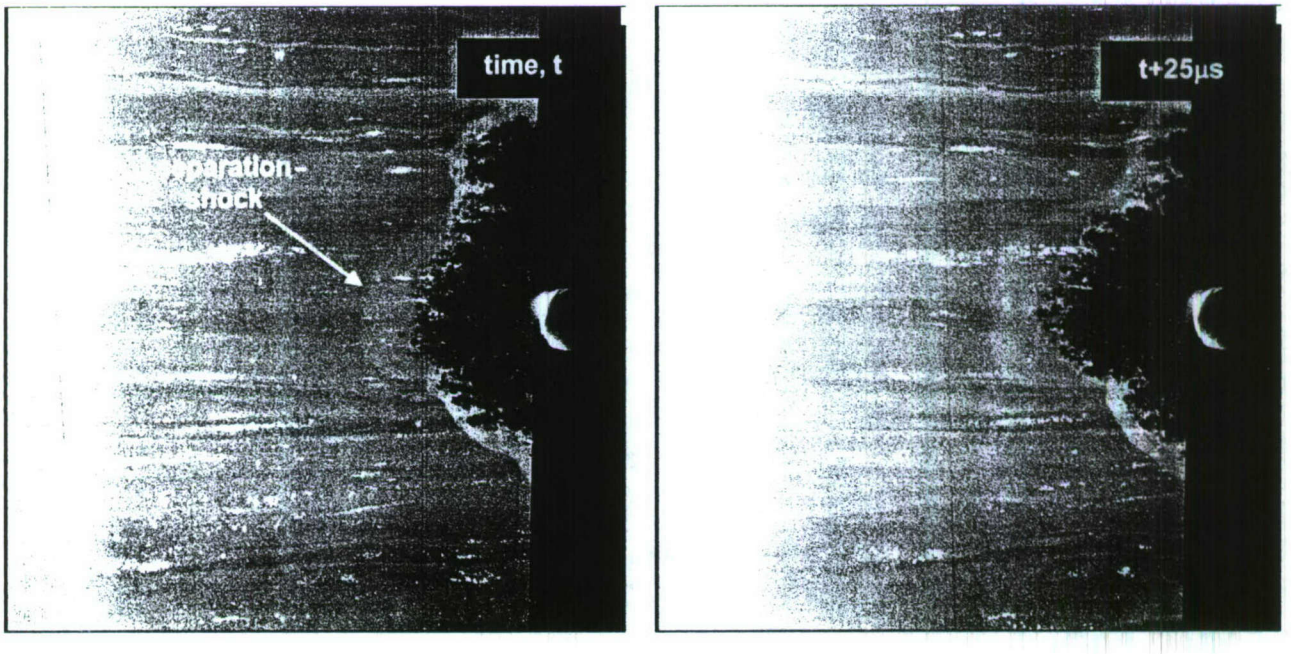

(b)

Figure 5. Two sample double-pulse plan-view PLS image pairs with cylinder at 2.8 inches. Time delay between first (left) and second (right) image is 25 microseconds. Flow is from left to right. (a) and (b) represent two examples of typical image pairs.

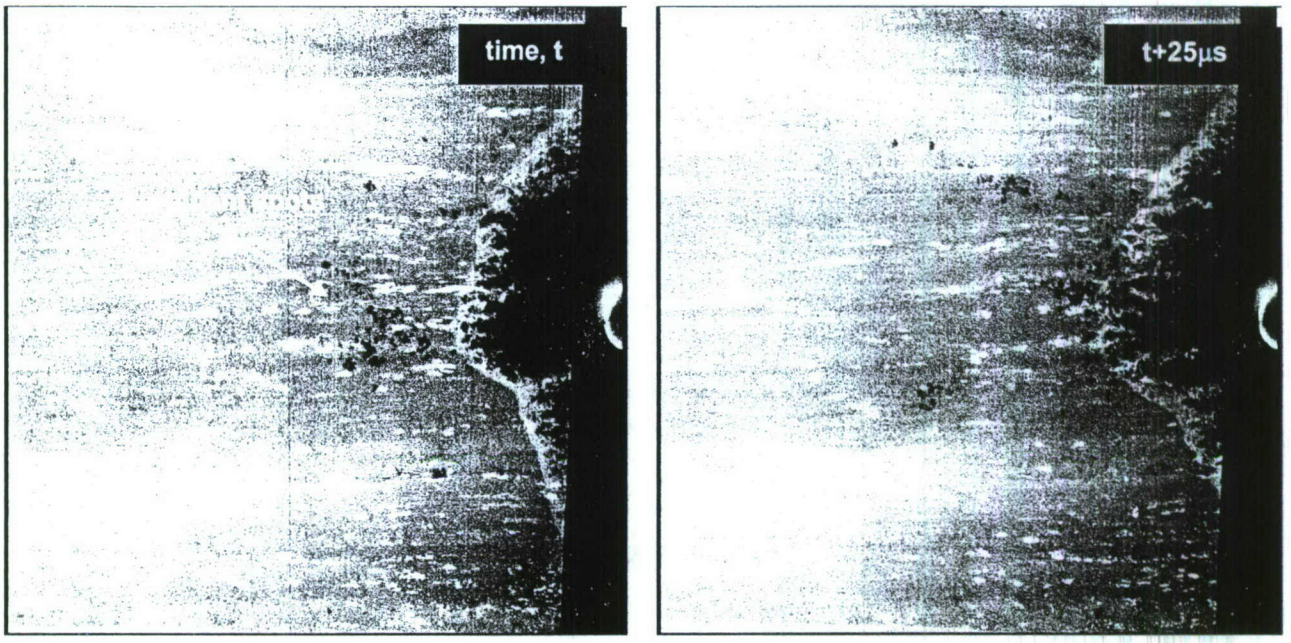

(a)

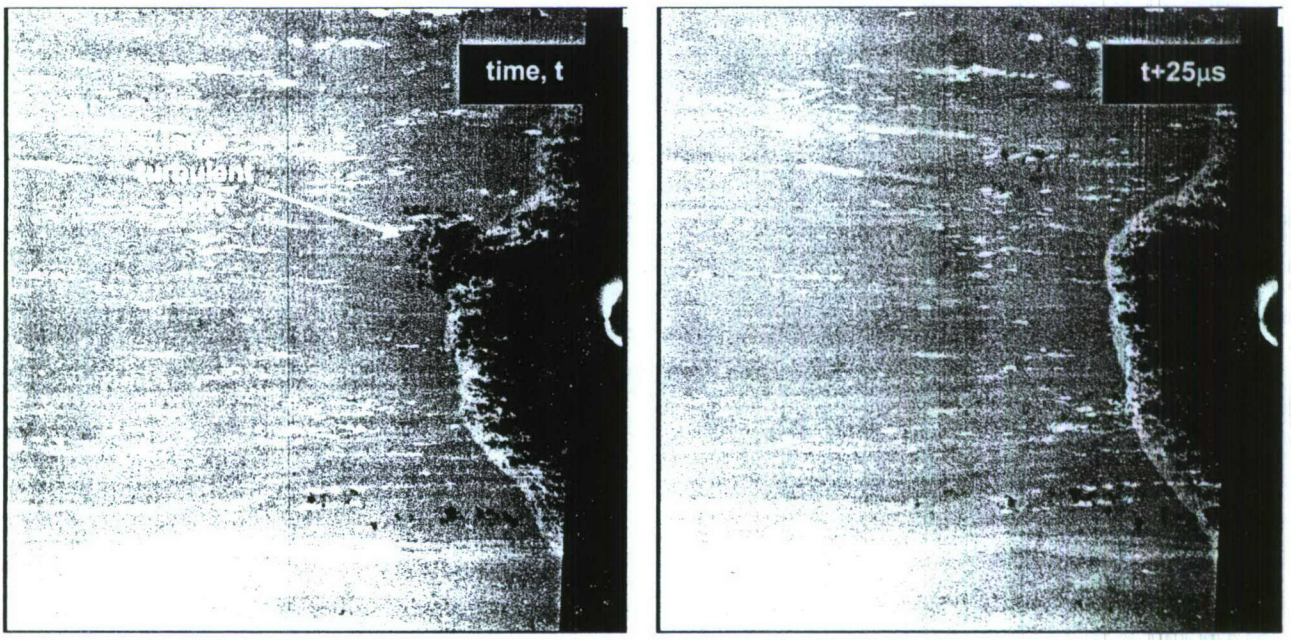

(b)

Figure 6. Two sample double-pulse plan-view PLS image pairs with cylinder at 2.8 inches. Time delay between first (left) and second (right) image is 25 microseconds. Flow is from left to right. (a) and (b) represent two examples of typical image pairs.

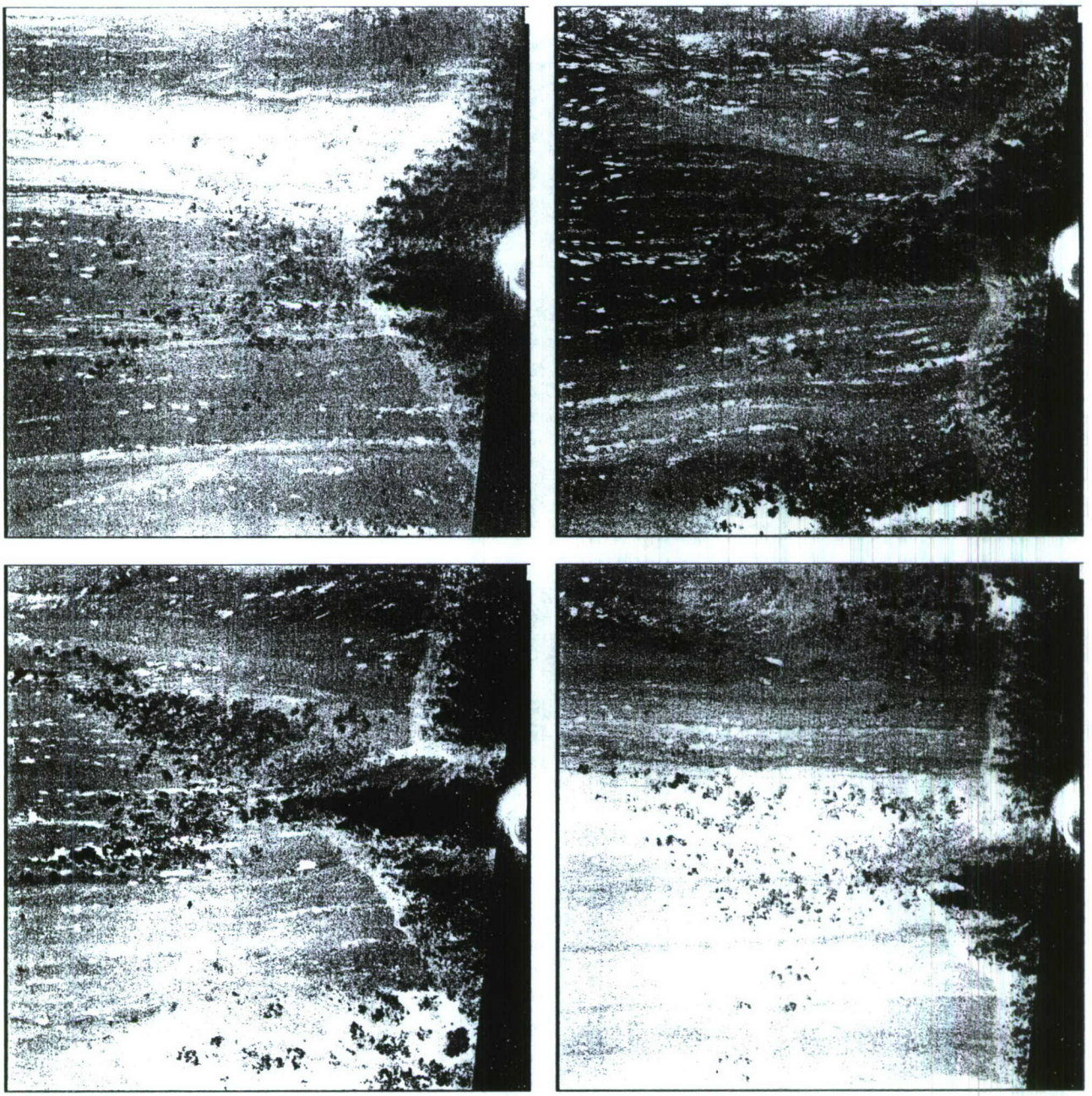

Figure 7. Sample PLS images with cylinder at 6.00 inches. Images are not image pairs; images are non-sequential.

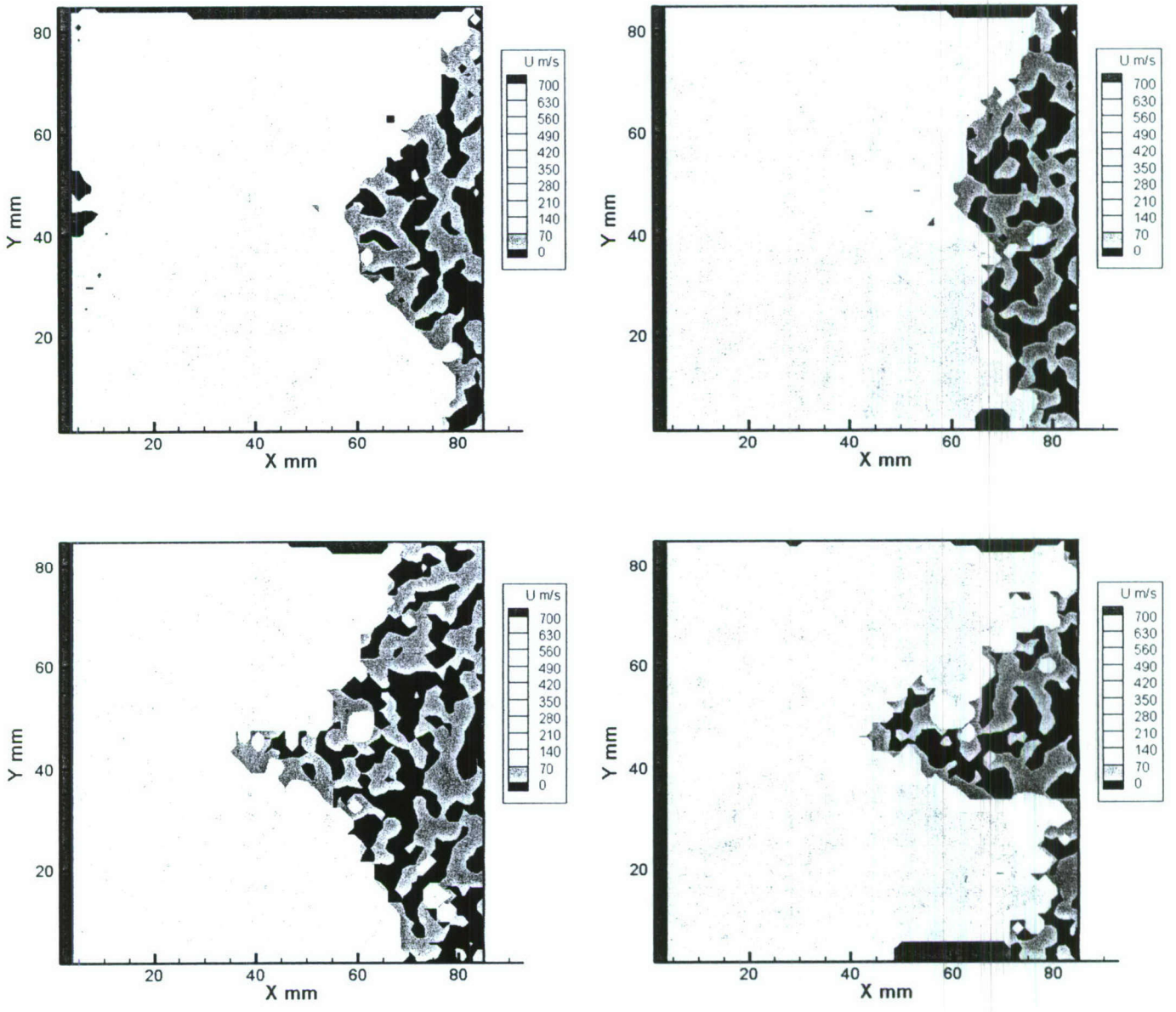

Figure 8. Streamwise velocity contours for interaction with cylinder at 6.0 inches. Images are non-sequential and were selected for similarities to respective PLS images in Figure 5.